THE JOURNAL OF BIOLOGICAL CHEMISTRY VOL. 280, NO. 49, pp. 40650–40659, December 9, 2005
Printed in the U.S.A.

Peroxisome Proliferator-activated Receptor γ Suppresses Proximal α1(I) Collagen Promoter via Inhibition of p300-facilitated NF-I Binding to DNA in Hepatic Stellate Cells*

Received for publication, September 14, 2005 Published, JBC Papers in Press, October 10, 2005, DOI 10.1074/jbc.M510094200

Sharon Yavrom[‡], Li Chen[‡], Shigang Xiong[‡], Jiaohong Wang[‡], Richard A. Rippe[§], and Hidekazu Tsukamoto[‡¶1]

From the [‡]Department of Pathology, Keck School of Medicine, University of Southern California, Los Angeles, California 90033, the [§]Department of Medicine, University of North Carolina, Chapel Hill, North Carolina 27599-7032, and the [¶]Department of Veterans Affairs Greater Los Angeles Healthcare System, Los Angeles, California 90073

Depletion of peroxisome proliferator-activated receptor γ (PPARγ) represents one of the key molecular changes that underlie transdifferentiation (activation) of hepatic stellate cells in the genesis of liver fibrosis (Miyahara, T., Schrum, L., Rippe, R., Xiong, S., Yee, H. F., Jr., Motomura, K., Anania, F. A., Willson, T. M., and Tsukamoto, H. (2000) *J. Biol. Chem.* 275, 35715–35722; Hazra, S., Xiong, S., Wang, J., Rippe, R. A., Krishna, V., Chatterjee, K., and Tsukamoto, H. (2004) *J. Biol. Chem.* 279, 11392–11401). In support of this notion, ectopic expression of PPARγ suppresses hepatic stellate cells activation markers, most notably expression of α1(I) procollagen. However, the mechanisms underlying this antifibrotic effect are largely unknown. The present study utilized deletion-reporter gene constructs of proximal 2.2-kb α1(I) procollagen promoter to demonstrate that a region proximal to −133 bp is where PPARγ exerts its inhibitory effect. Within this region, two DNase footprints with Sp1 and reverse CCAAT box sites exist. NF-I, but not CCAAT DNA-binding factor/NF-Y, binds to the proximal CCAAT box in hepatic stellate cells. A mutation of this site almost completely abrogates the promoter activity. NF-I mildly but independently stimulates the promoter activity and synergistically promotes Sp1-induced activity. PPARγ inhibits NF-I binding to the most proximal footprint (−97/−85 bp) and inhibits its transactivity. The former effect is mediated by the ability of PPARγ to inhibit p300-facilitated NF-I binding to DNA as demonstrated by chromatin immunoprecipitation assay.

Cirrhosis, the advanced stage of liver fibrosis, is the 12th leading cause of medial mortality in 2002 with 27,257 annual deaths according to a report by the Center for Disease Control. This mortality is even higher among those with productive ages between 45 and 54, ranking it as the fourth leading cause of death, highlighting medical and socioeconomic significance of the disease (1). Currently, there is no medical treatment for the disease other than liver transplantation. Therefore, the understanding of cellular and molecular mechanisms of liver fibrogenesis is of primary importance for the development of new treatments. The effector cell type for liver fibrosis is the hepatic stellate cell (HSC).[2] HSCs are liver mesenchymal cells that are believed to function as pericytes for the liver microcirculatory system called sinusoids. They are located in the perisinusoidal space, an anatomical area nestled between the nonluminal surface of the sinusoidal endothelial cell and the microvilli surface of the hepatocyte (2). HSCs constitute 7–10% of the liver cell population and it stores 85% of the body's total vitamin A content (3, 4). They also produce and maintain the normal matrix milieu (basement membrane components) of the perisinusoidal space. In addition, HSC provides direct and indirect homeostatic control over hepatocytes through communication via gap junctions (5) and the release of soluble factors such as hepatocyte growth factor (6), epimorphin (7), and pleiotrophin (8). However, these cells are also responsible for a severalfold increase in the production of extracellular matrix components in the genesis of liver fibrosis (4).

Upon fibrogenic stimulation, quiescent HSCs transdifferentiate to myofibroblastic cells to produce excessive extracellular matrix. This cellular transition process is characterized by the loss of vitamin A storage; cellular proliferation and migration; acquisition of a myofibroblastic phenotype, such as expression of α smooth muscle actin, induction of fibrogenic extracellular matrix genes (collagen type I and III), expression of autocrine cytokines, such as platelet-derived growth factor (9), transforming growth factor α, transforming growth factor β (10–13), and their receptors; and expression of adhesion molecules (intercellular adhesion molecules); and chemokines (MCP-1, CINC) (14). In search of the molecular basis of this unique HSC transdifferentiation phenomenon, we and others recently disclosed that this process is accompanied by reduced levels of a member of the nuclear hormone receptor family, peroxisome proliferator-activated receptor γ (PPARγ) (15, 16). Further, our subsequent studies demonstrated that this molecular "defect" in transdifferentiated HSC is part of the loss of adipogenic transcriptional program required for the maintenance of HSC quiescence (17). In fact, this loss of the adipogenic program and the transdifferentiation process are coordinately reversed by ectopic expression of PPARγ (18) or sterol regulatory element-binding protein 1c (17), another key adipogenic transcription factor.

One of the most pivotal antifibrotic effects of PPARγ is its ability to inhibit type I collagen expression at the level of the transcription (15, 16). Type I collagen makes up 40–50% of the total collagen proteins in the normal liver and is increased to 60–70% in the cirrhotic liver (3). Type I collagen is a heterotrimeric protein composed of two α1(I) and one α2(I) collagen polypeptides encoded by two different genes that are coordinately up-regulated in liver fibrogenesis (19). Treatment of activated HSC with a ligand for PPARγ (15, 16) or transduction of these cells with a PPARγ plasmid (15, 16) represses basal α1(I) procollagen promoter activity that is largely dependent on a proximal 2.2-kb 5′-flanking region (19, 20). However, the mechanism by which PPARγ

* The costs of publication of this article were defrayed in part by the payment of page charges. This article must therefore be hereby marked "*advertisement*" in accordance with 18 U.S.C. Section 1734 solely to indicate this fact.

[1] To whom correspondence should be addressed: Keck School of Medicine of the University of Southern California, 1333 San Pablo St., MMR-402, Los Angeles, CA 90033-9141. Tel.: 323-442-5107; Fax: 323-442-3126; E-mail: htsukamo@usc.edu.

[2] The abbreviations used are: HSC, hepatic stellate cell; PPARγ, peroxisome proliferator-activated receptor γ; PPRE, peroxisome proliferator-activated receptor response element; CBP, CREB-binding protein; CREB, cAMP-response element-binding protein; FP, footprint; GFP, green fluorescent protein; EMSA, electrophoretic mobility shift assay; ChIP, chromatin immunoprecipitation; BSC, biliary fibrosis-derived stellate cell.

This is an Open Access article under the CC BY license.

inhibits type I collagen promoter activity is currently unknown. The present study investigated where in the proximal 2.2 kb α1(I) procollagen promoter PPARγ renders its inhibition and how it achieves this effect. Our results demonstrate that the 5′-flanking α1(I) procollagen promoter proximal to −133 bp is where PPARγ renders its inhibitory effect. This inhibition is mediated by the ability of PPARγ to suppress NF-I binding and transactivity via inhibition of p300-facilitated NF-I binding.

MATERIALS AND METHODS

HSC Isolation and Cell Culture—HSCs were isolated from normal male Wistar rats as previously described (21). Briefly, nonparenchymal cells were isolated via sequential digestion with Pronase and type IV collagenase, followed by differential low speed centrifugation. A pure fraction of HSC was isolated by arabinogalactan gradient ultracentrifugation and collecting the cells at the interface between the medium and a 1.035 density gradient. Cell purity was determined using phase-contrast microscopy and UV-excited fluorescence microscopy. Cell viability was determined by trypan blue exclusion. Cells were cultured on a 100-mm dish in low glucose Dulbecco's modified Eagle's medium supplemented with 10% fetal bovine serum, 100 mg/ml streptomycin, 10,000 units/ml penicillin, and 25 μg/ml amphotericin B. Cells were maintained in the culture medium for 7 days, at which time adenoviral vectors were added. Spontaneously immortalized, activated HSCs were established from a rat with cholestatic liver fibrosis and termed as biliary fibrosis-derived stellate cells (BSCs) (22). These cells have the phenotype similar to activated HSC. BSCs were cultured in 10% low glucose medium and primarily used in transient transfection experiments.

Adenoviral Vector Infection—Full-length PPARγ1 cDNA was cloned from pCMX-PPARγ1 into the transfer vector, subsequently allowing homologous recombination with the pAdEasy-1 adenoviral plasmid containing a green fluorescent protein (GFP) reporter (Stratagene, La Jolla, CA) as previously described (18). A control vector containing cytomegalovirus-driven GFP reporter gene was also constructed. On the seventh day of primary rat HSC culture, a vector was applied to HSCs at a multiplicity of infection of 100 to infect and transduce PPARγ or GFP. The following day, the medium was changed, and the cells were cultured for an additional four days to observe the effects on HSC as described (18).

RNA Isolation and Quantitative Real Time PCR—Total RNA was extracted from isolated HSC transduced with Ad.GFP and Ad.PPARγ using Trizol reagent (Invitrogen). Two nanograms of total RNA was used in a 20-μl reaction with reverse transcriptase for 30 min followed by 40 cycles of PCR to produce products using TaqMan Gold One Step PCR Kit (Applied Biosystems, Foster City, CA) and the ABI 7700 SDS thermocycler (Applied Biosystems). Synthesized cDNA was amplified using specific primers for α1(I) collagen (5′-TCGATTCACCTACAGCACGC, 5′-CATTAGCATCCGTGGGAACA), glyceraldehyde-3-phosphate dehydrogenase (5′-TGCACCACCAACTGCTTAG, 5′-GGATGCAGGGATGATGTTC). Probes were 5,6-carboxylfluorescein amidite labeled at the 5′-end and black hole quencher-1 labeled at the 3′-end (Biosearch Technologies Inc., Novoato, CA).

Plasmids and Transient Transfection—pCMX and pCMX-PPARγ were gifts from Ron Evans (The Salk Institute, La Jolla, CA). pSG5 and p300 were gifts from Michael Stallcup (University of Southern California). Mouse collagen promoter deletion constructs were as follows: pCol2-lucif, pCol3-lucif, pCol6-lucif, pCol7-lucif, and pUC-Cat (−220, −133, −120, and −92 bp/+115 bp) were used as previously described (19, 20). pPac, pPac-NF-I and pPac-Sp1 were used to assess the effects of PPARγ on NF-I- or Sp1-driven promoter activity. *Renilla* pRL-TK was purchased from Promega. Luciferase promoter deletion constructs were created via restriction enzyme digestion (XbaI and XhoI) of the pUC-Cat constructs and insertion into the pGL3-luciferase (Promega) backbone. Briefly, BSC or NIH3T3 cells were seeded in 6- or 24-well plates and incubated overnight. A collagen promoter construct, an expression plasmid (pCMX or PPARγ), and F2 reagent (Targeting System, San Diego, CA) were mixed and added to serum-free, high glucose Dulbecco's modified Eagle's medium and incubated for 25 min at 37 °C and then placed onto the cells. Two hours later, the cells were supplemented with 10% high glucose Dulbecco's modified Eagle's medium. The following day, the medium was changed, and the cells were incubated for an additional 8 h. The cell lysates were collected using 5× passive lysis buffer (Promega) and dual luciferase assay (Promega) was performed using a luminometer (E&G Berthold). Mutations of three nucleotides (TGG to CAA) in the most proximal reverse CCAAT box was created by site-directed mutagenesis according to the QuikChange™ protocol (Stratagene). Primers were designed to introduce 3-nucleotide mutations into the wild type CCAAT of the FP-1 region of the luciferase promoter deletion construct (−133 bp/+115 bp). The DNA sequence of each construct was verified using an ABI Prism 377 sequencer (PerkinElmer Life Sciences). The following primers were used: FP-1-mutant NF-I (forward), 5′-gggccaggcagttctgatCAActgggggccgggctgctggctc-3′; FP-1-mutant NF-I (reverse), 5′-gagccagcagcccggcccccagTTGatcagaactgcctggccc-3′.

Electrophoretic Mobility Shift Assay—Nuclear proteins were extracted from HSC infected with Ad.GFP or Ad.PPARγ using Dignam A and C reagents (23). Extracts (5–10 μg) were incubated in a reaction mixture (20 mM HEPES, pH 7.6, 100 mM $MgCl_2$, 0.2 mM EDTA, 2 mM dithiothreitol, 20% glycerol, 200 μg/ml poly(dI-dC)) on ice for 10 min followed by an additional 20-min incubation on ice with 2 ng of α-^{32}P-labeled double-stranded oligonucleotides as described below: ARE-7, 5′-GCTTACTGGATCAGAGTTCACAGAT; FP-1, 5′-GATTGGCTGGGGGCCGGGCTGCT; FP-2, 5′-GGTTCCAAATTGGGGGCCGGGCCAG; Sp1, 5′-GATCAATGGGGCGGGGCAAT; NF-I, 5′-GGTTTTGGATTGAAGCCAATATGAG.

The reaction mixture was resolved on a 6% nondenaturing polyacrylamide gel (Bio-Rad) in 0.5× TBE (45 mM Tris, 45 mM boric acid, 1 mM EDTA). The gel was dried and subjected to phosphorimaging for detection of shifted bands. For a supershift analysis, polyclonal antibodies against NF-I, Sp1, or Sp3 (Santa Cruz Biotechnology, Inc., Santa Cruz, CA) were added and incubated on ice for an additional 30 min. For competition analysis, a 200-fold molar excess of a cold probe was added to the reaction mixture just prior to the addition of α-^{32}P-labeled probe.

Chromatin Immunoprecipitation (ChIP) Assay—The ChIP assay was performed using the ChIP assay kit according to the manufacturer's protocol (Upstate Biotechnology, Inc., Lake Placid, NY). In brief, ChIP assay was performed on HSC cultured on plastic for 7 days or NIH3T3 cells without or with transfection with NF-I, PPARγ, and/or p300 expression plasmids or respective empty vectors. After a 48-h incubation, ~4×10^6 cells/ChIP assay, were cross-linked with 1% formaldehyde at 37 °C for 10 min and rinsed twice with ice-cold phosphate-buffered saline. The cells were harvested by brief centrifugation and lysed in SDS-lysis buffer (50 mmol/liter Tris-HCl, pH 8.1, 10 mmol/liter EDTA, 1% SDS, protease inhibitors). The lysates were sonicated on ice with two pulses at 15 s each to achieve chromatin fragments ranging between 200 and 1000 bp in size followed by centrifugation at 15,000 rpm for 10 min at 4 °C. Supernatants were collected and diluted 10-fold in a ChIP dilution buffer (a 20-μl aliquot was removed to serve as an input sample) followed by preimmunoprecipitation clearing with 80 μl of a mixture of salmon sperm DNA/Protein A at 4 °C with rotation for

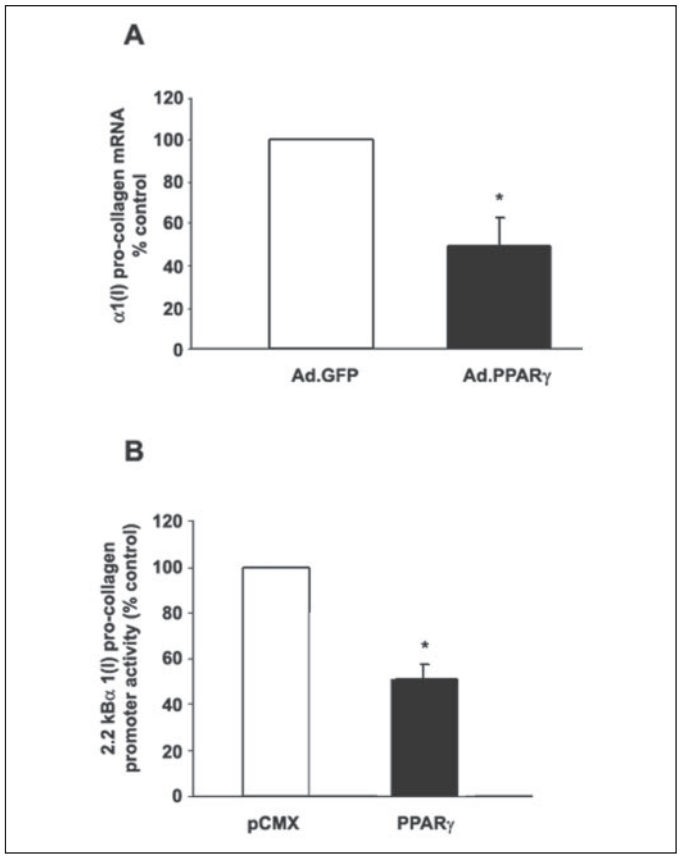

FIGURE 1. **PPARγ suppresses α1(I) procollagen mRNA expression and 2.2-kb collagen promoter activity.** *A*, Taqman reverse transcription-PCR analysis shows that PPARγ expression in culture-activated HSCs by an adenoviral vector (Ad.PPARγ) reduces α1(I) procollagen mRNA level by 50%. *, $p < 0.05$ as compared with HSC transduced with the control GFP vector (Ad.GFP) ($n = 6$ pairs). *B*, a transient transfection experiment using a PPARγ expression vector and a 2.2-kb collagen promoter-luciferase construct demonstrates a 50% inhibition of the promoter by PPARγ as compared with the cells transfected with an empty vector (pCMX). *, $p < 0.05$ as compared with the cells transfected with pCMX ($n = 5$ pairs).

30 min. Immunoprecipitation was carried out with 1 μg of antibodies (anti-NF-I, anti-p300, and anti-CCAAT DNA-binding factor (CBF)/NF-Y antibodies from Santa Cruz Biotechnology) at 4 °C overnight with rotation. After immunoprecipitation, 60 μl of a mixture of salmon sperm DNA and Protein A was added and incubated at 4 °C with rotation for 30 min and followed by brief centrifugation. The precipitates were washed twice with low salt buffer, once with high salt buffer, and once with LiCl buffer. Then the precipitates were washed again with the TE buffer. The immune complexes were extracted twice with 250 μl of elution buffer. The extracted complexes and the input were heated at 65 °C for 4 h after the addition of 20 μl of 5 mol/liter NaCl to reverse cross-link. Following proteinase K treatment, DNA was extracted by phenol/chloroform solution and precipitated with 20 μg of glycogen. The recovered DNA was resuspended and subjected to 35 cycles of PCR using the following primers: α1(I) procollagen promoter FP-1 region, 5′-TGGACTCCTTTCCCTTCCTTTCCCTCCT-3′ and 5′-TGGGCCCCTTTTATACCATC-3′; aP2 gene PPRE region, 5′-TGCACATTTCACCCAGAGAG-3′ and 5′-TGTTTGGGCTGTGACACTTC-3′. The PCR products were analyzed on 1.5% agarose gel.

RESULTS

PPARγ Inhibits α1(I) Procollagen mRNA Expression and Promoter Activity—PPARγ is depleted in activated HSC, whereas activation markers including the α1(I) collagen gene are induced (15, 16). Ectopic expression of PPARγ in culture-activated HSC by an adenoviral vector reduces the level of α1(I) procollagen mRNA by half as compared with HSC transduced with a control GFP vector as determined by real time PCR (Fig. 1*A*). Transient transfection experiment using the HSC cell line (BSC cells) reveals that PPARγ expression also decreases by 50% the activity of a proximal 2.2-kb α1(I) procollagen promoter known to encompass the highest basal activity in fibroblasts (19, 20) (Fig. 1*B*). These results confirm the previous finding (15, 16, 18) and further support that the inhibitory effect of PPARγ is at the level of the proximal promoter.

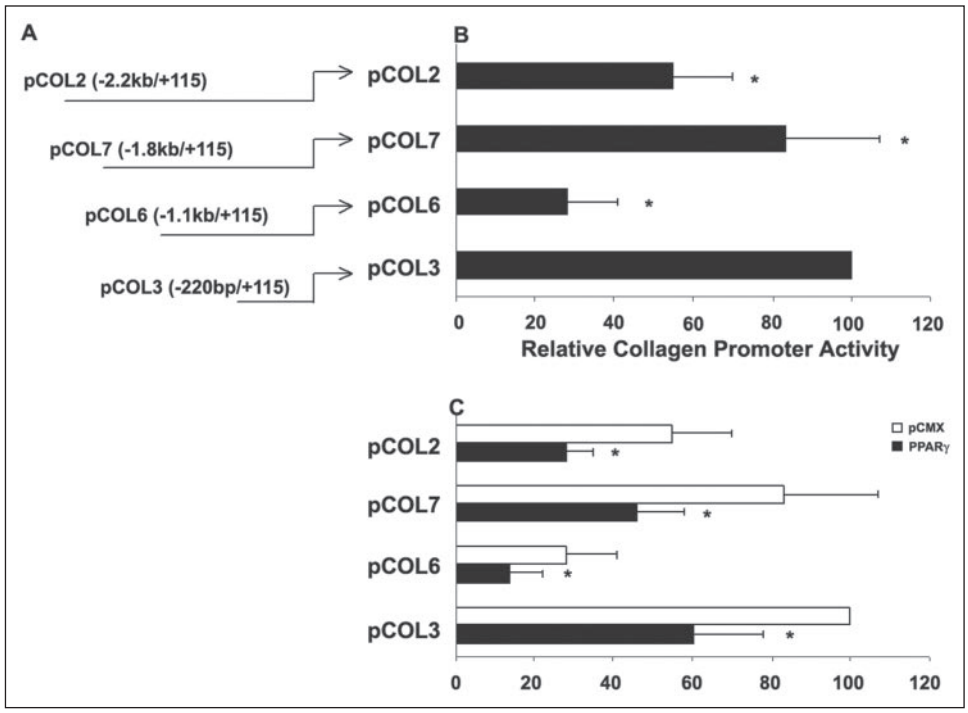

FIGURE 2. **PPARγ suppresses the collagen promoter within the −220 bp proximal promoter region.** *A*, a schematic diagram of four deletion constructs within the proximal 2.2 kb α1(I) collagen promoter. *B*, relative promoter activities of the collagen promoter deletion constructs as compared with the highest activity achieved by the −220/+115 bp promoter. *, $p < 0.05$ as compared with the activity of pCOL3 ($n = 4$). *C*, PPARγ equally inhibits each deletion construct by 50%, suggesting that the primary site of the inhibitory effect of PPARγ is located within the −220 bp collagen promoter region. *, $p < 0.05$ as compared with pCMX-transfected cells ($n = 4$).

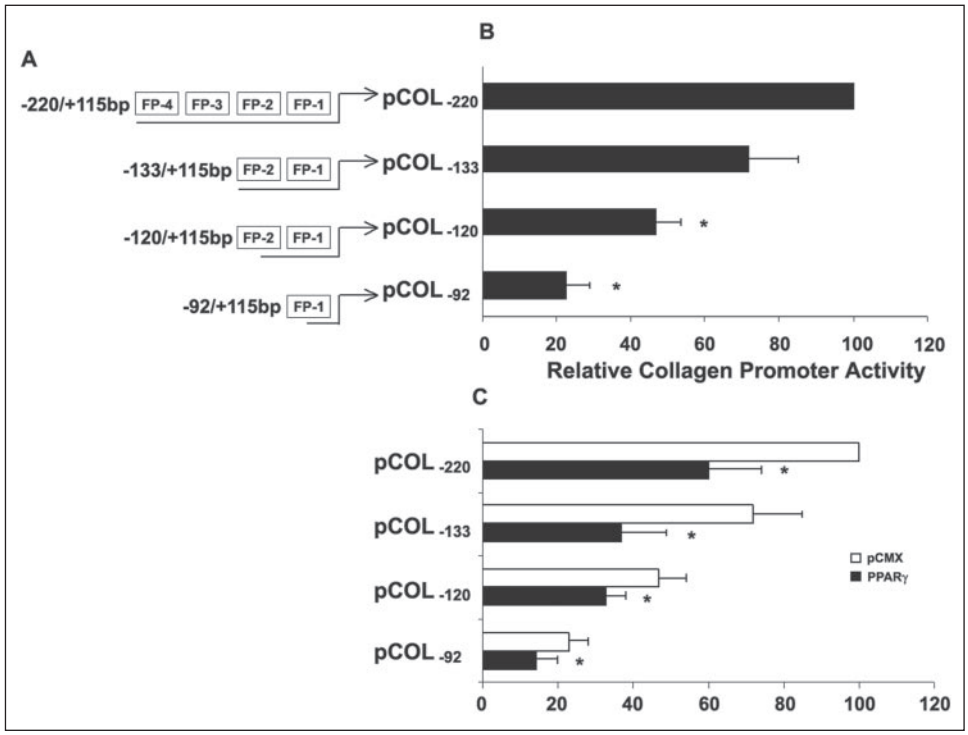

FIGURE 3. **PPARγ inhibits the proximal 220 bp collagen promoter at the FP-1 and FP-2 sites.** *A*, a schematic diagram of deletion constructs within the −220 bp α1(I) collagen promoter in reference to the known four DNase footprints. *B*, relative activities of the collagen promoter deletion constructs transfected in BSCs. *, $p < 0.05$ as compared with pCOL−220 ($n = 5$). *C*, co-transfection experiments using deletion constructs and a PPARγ expression vector reveals that PPARγ inhibits the −220 and −133 bp promoters by 45–50%, but this inhibition is attenuated when FP-2 is disrupted in pCOL-120. PPARγ still suppresses pCOL-92 containing the proximal portion of FP-1. *, $p < 0.05$ as compared with pCMX-transfected cells ($n = 5$–7).

A Site of the Inhibitory Effect of PPARγ Is Located within the Most Proximal −220 bp α1(I) Collagen Promoter Region—In order to assess the region within the 2.2-kb promoter that is subjected to PPARγ-mediated inhibition, we performed transient transfection experiments using four deletion constructs of the promoter (Fig. 2*A*). The relative activity of each of the deletion constructs was tested first by transfection experiments in BSCs (Fig. 2*B*). Our results reveal that two repressor elements: one between −2.2 and −1.8 kb and another between −1.1 and −220 bp. An enhancer element is also found between −1.8 and −1.1 kb. Of all four deletion constructs, the region proximal to −220 bp is shown to have the highest promoter activity in consistent with the previous findings (19, 20). Co-transfection of each deletion construct with a PPARγ or empty vector reveals that PPARγ inhibits all of the deletion constructs by ~50% (Fig. 2*C*). Since the −220 bp region has the highest activity and PPARγ expression equally reduces the activity of each promoter construct, we concluded that PPARγ primarily exerts its inhibitory effect within the −220 bp proximal region and +115 bp of the first exon. Our review of the −220 bp proximal promoter sequence fails to reveal a PPRE. Thus, PPARγ must mediate the effect not via direct repression but via its interaction with other *trans*-acting factor(s) and/or *cis*-regulatory element(s).

Inhibition of PPARγ Is Confined to DNase Footprint (FP)-1 and -2 Regions within the −133 bp α1(I) Collagen Promoter—To further define the site of PPARγ-mediated inhibition, we designed and created an additional set of deletion constructs within the most proximal −220 bp region. This region is known to contain four protected footprints as determined by DNase footprinting analysis of activated HSC (24) (Fig. 3*A*), and newly created deletions are designed to test these FP regions: −133/+115 (FP-3 and FP-4 deleted but intact FP-2 and -1); −120/+115 (distal region of FP-2 deleted but intact FP-1); and −92/+115 bp (only proximal region of FP-1). Transient transfection experiments reveal that the two distal footprints (FP-3 and FP-4) contribute minimally to basal collagen promoter activity (a statistically significant change in the promoter activity is not attained by this deletion: pCOL−133) (Fig. 3*B*). However, an additional deletion, including the distal half of FP-2 reduces the basal promoter activity to 50%, and a further deletion within FP-1 reduces the promoter activity by another 50%. Overexpression of PPARγ expression vector results in a 50% inhibition on the pCOL−133 promoter (Fig. 3*C*). This effect is attenuated when FP-2 is disrupted (pCOL-120). PPARγ also retains a modest inhibitory effect on the promoter activity rendered only by the most proximal portion of the FP-1 (pCOL-92). However, the absolute magnitude of the activity inhibited by PPARγ accounts only for 25% of the inhibition seen with pCOL−220 or pCOL−133. These results suggest that both FP-1 and FP-2 contain the sites via which PPARγ renders a major inhibitory effect on the promoter.

PPARγ Inhibits NF-I Binding to FP-1 but Has No Effects on Sp1 Binding to FP-2—Since FP-1 and FP-2 are shown to be the most likely sites of the inhibitory action of PPARγ, we next investigated what *trans*-acting factors bind to these regions in activated HSC. NF-I and Sp1 are shown to comprise protein components that bind to FP-1 in NIH3T3 fibroblasts (19) and activated HSC (20). We used electrophoretic mobility shift assays (EMSA) to characterize these DNA-protein interactions of FP-1 in activated HSC. Using nuclear extracts from culture-activated HSC and a radiolabeled oligonucleotide probe containing the FP-1 sequence, one major DNA-protein complex and another faint, higher molecular weight band are detected. To identify proteins bound to FP-1, supershift assays were performed using antibodies against NF-I, Sp1, and Sp3. Although a supershifted band is not detected, NF-I antibody clearly diminishes the major band and Sp1 antibody abrogates only the upper, faint band. Sp3 antibody fails to affect either band (Fig. 4*A*). The addition of a cold consensus NF-I binding sequence in excess, completely eliminates the protein binding to the FP-1 probe, as does the cold FP-1 probe (Fig. 4*C*). The addition of a cold Sp1 consensus element in excess eliminates the upper protein-DNA complex without affecting the lower major band (Fig. 4*C*). These results demonstrate that the lower major band of DNA-protein complex contains NF-I, and the upper band contains Sp1 and maybe NF-I.

We also performed EMSA to determine proteins bound to the FP-2 DNA. Using nuclear extracts from activated HSC and a FP-2 probe, two DNA-protein bands are identified. Supershift assays reveal that Sp1

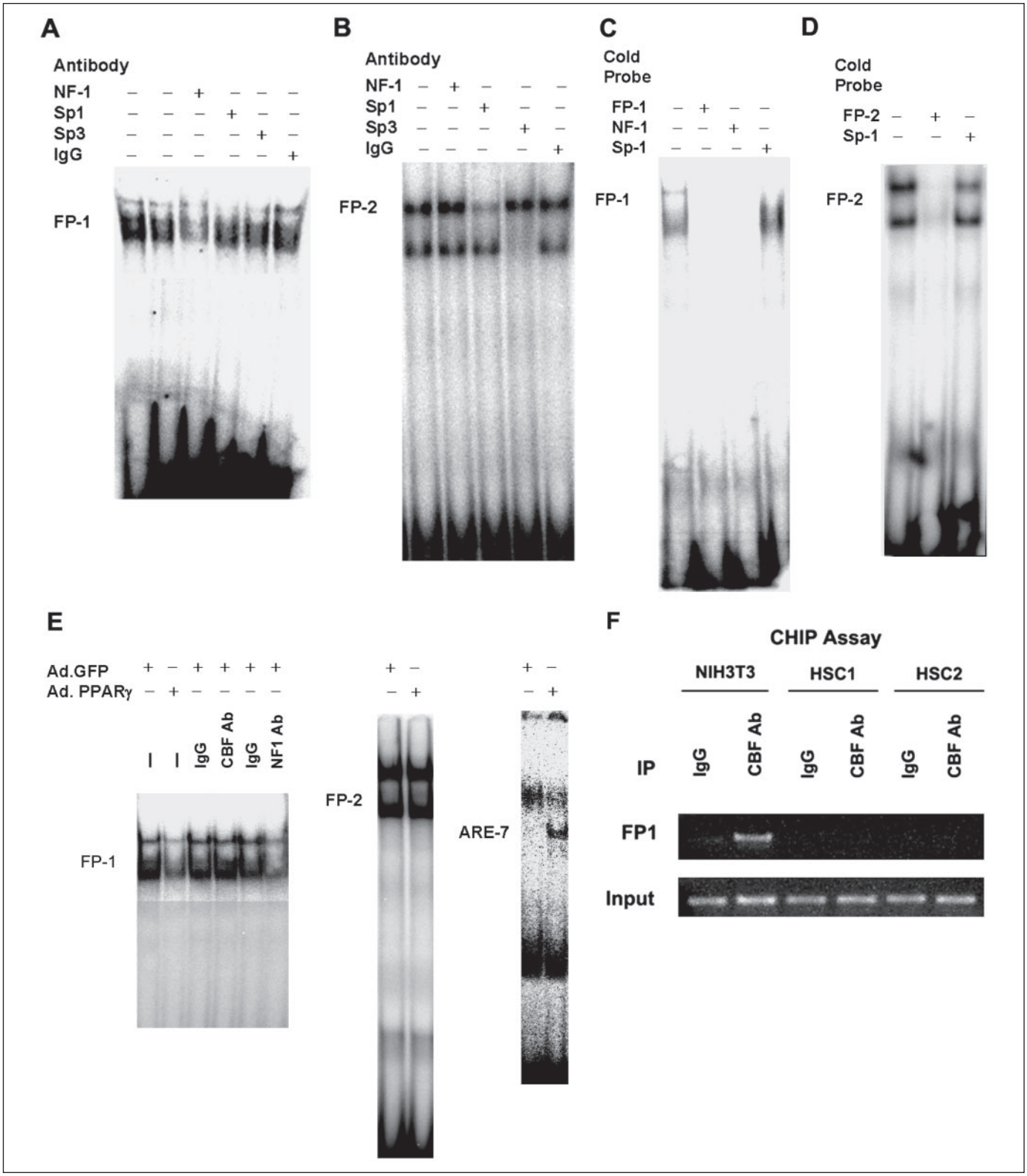

FIGURE 4. **PPARγ reduces the binding of NF-I to FP-1 but not that of Sp1 or Sp3 to FP-2.** *A* and *B*, supershift assays with antibodies determine that NF-I is a major protein that binds to FP-1, with Sp1 being a minor component. Both Sp1 and Sp3 bind to FP-2. *C* and *D*, cold probe competition confirms protein binding to FP-1 and FP-2. *E*, forced PPARγ expression reduces NF-I binding to FP-1 (*left panel*) while having no effects on Sp1 and Sp3 binding to FP-2 (*middle panel*). NF-I binding is confirmed by abrogation of protein-DNA complex formation with anti-NF-I antibody (*last lane* of the *left panel*), whereas CBF binding is not evident by the lack of effect with anti-CBF antibody (*Ab*) (*fourth lane* of the *left panel*). PPARγ overexpression is validated by increased binding to an ARE-7 probe (a PPRE probe from the aP2 gene (*right panel*)). *F*, ChIP assay reveals CBF binding to FP-1 in NIH3T3 cells but not in HSC (HSC1 and HSC2). *IP*, immunoprecipitation.

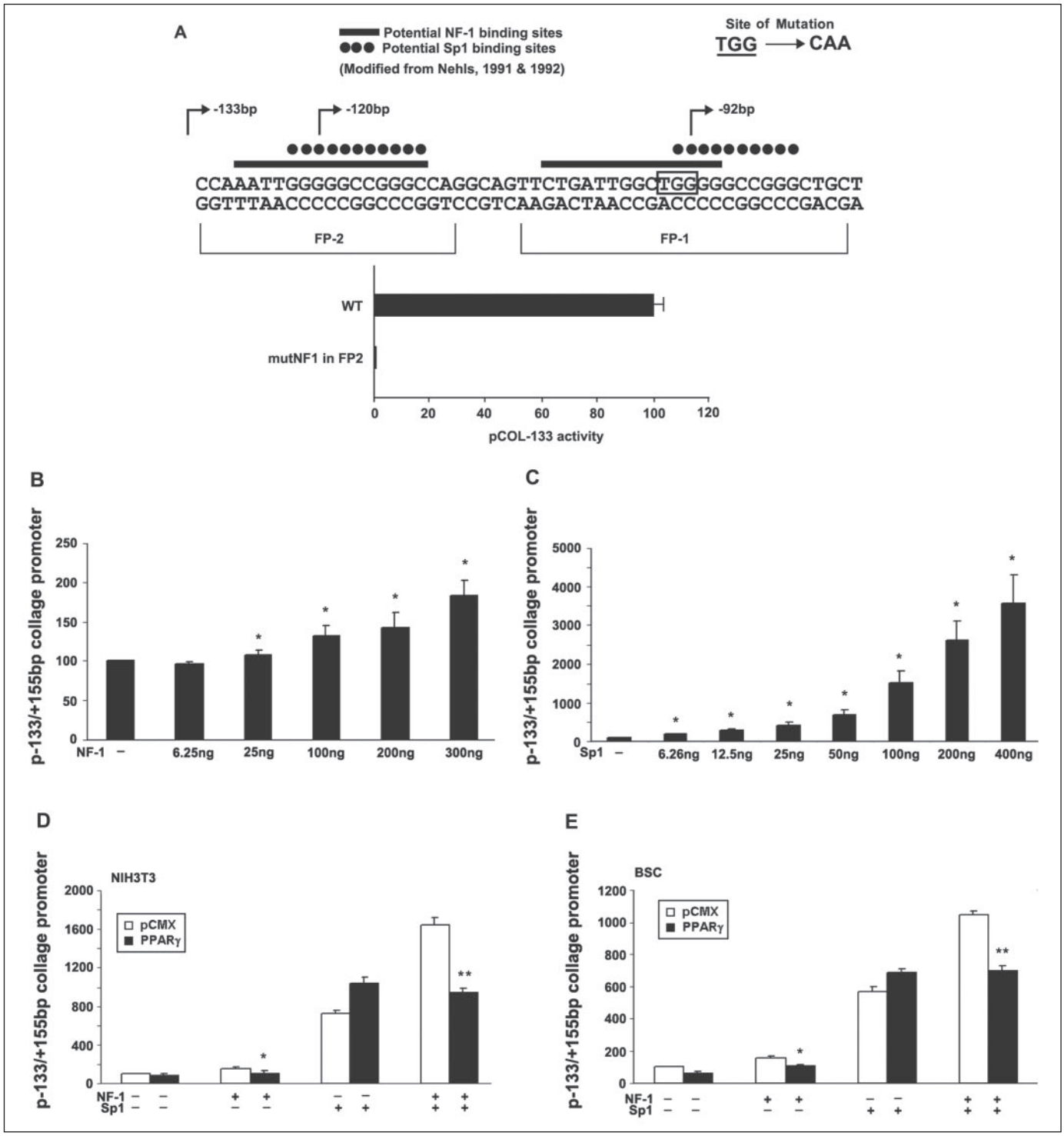

FIGURE 5. **PPARγ inhibits NF-I-mediated collagen promoter activity and NF-I/Sp1-mediated synergistic activation of the promoter.** *A*, a schematic drawing of the DNA sequences of FP-1 and FP-2 of the α1(I) collagen promoter with reverse CCAAT binding sites and two identical 12-bp GC repeats. It also shows the site of mutation within the proximal CCAAT site in FP-1. These 3-nucleotide mutations result in an almost complete loss of the pCOL−133 promoter activity as compared with the wild type (*WT*) promoter, as shown by transient transfection in BSCs. *B*, NF-I modestly but dose-dependently stimulates the collagen promoter activity in NIH3T3 cells. *, $p < 0.05$ as compared with the control ($n = 4$). *C*, Sp1 conspicuously induces the collagen promoter activity in a dose-dependent manner. *, $p < 0.05$ as compared with the control ($n = 4$). *D*, PPARγ inhibits NF-I-mediated collagen promoter activity (*, $p < 0.05$, $n = 5$), and it also suppresses NF-I/Sp1 mediated synergistic induction of the collagen promoter (**, $p < 0.05$, $n = 5$) in NIH3T3 cells. *E*, the similar inhibitory effects of PPARγ are observed in BSCs.

antibody diminishes the upper band, whereas Sp3 antibody completely abrogates the lower band (Fig. 4*B*). NF-I antibody has no effects. The addition of a cold consensus Sp1 binding element in excess completely eliminates the upper band, whereas an excess amount of unlabeled FP-2 decreases both *upper* and *lower bands* (Fig. 4*D*). Thus, these results demonstrate that the upper DNA-protein complex contains Sp1, a 105/95-kDa protein, and the lower band contains Sp3, an 80-kDa protein, in activated HSC.

Next, we tested whether expression of PPARγ affects the binding of the nuclear proteins to FP-1 and FP-2. We performed EMSA using

nuclear extracts from activated HSC infected with either Ad.PPARγ or Ad.GFP. Our results show that PPARγ does not affect protein binding to FP-2 (Fig. 4*E*, *middle panel*) but reduces the intensity of complexes formed with the FP-1 that contain NF-I (*second lane* of the *left panel*) (Fig. 4*E*). A PPARγ-specific DNA binding sequence, ARE-7, was used to confirm increased binding of PPARγ by the nuclear extracts of the Ad.PPARγ-infected cells (Fig. 4*E*, *right panel*). CBF/NF-Y binds to a CCAAT box in the proximal murine α2(I) procollagen promoter in NIH3T3 cells (25–27). Thus, the binding of this factor to a reverse CCAAT site in FP-1 of α1(I) collagen promoter is possible. To test this, we first used anti-CBF antibody for EMSA with the FP-1 probe and HSC nuclear extracts. As shown in the *fourth lane* of the *left panel* of Fig. 4*E*, this antibody does not affect the DNA-protein complex formation, whereas anti-NF-I antibody clearly decreases it (*last lane*). Using the same antibody, we also performed a ChIP assay. For this, we used both NIH3T3 cells and HSC spontaneously activated in culture on plastic. CBF binding to FP-1 was evident in NIH3T3 cells but not in HSC (Fig. 4*F*). These results demonstrate that CBF does not bind to the reverse CCAT site in FP-1 in HSC.

NF-I Is Most Important for Proximal α1(I) Procollagen Promoter Activity—The above data suggest that NF-I is a likely target of PPARγ. To better understand the functional importance of NF-I in the context of the promoter of interest, 3 nucleotides in the reverse CCAAT site of FP-1 that is shown to be critical for NF-I binding (19) were mutated (−98/−96; TGG → CAA), and the activity of the mutated pCOL−133 promoter was assessed in BSCs. As shown in Fig. 5*A*, this mutation almost completely abrogates the promoter activity. Because of very low promoter activity of the mutated promoter, the effect of PPARγ could not be assessed. Nonetheless, this result demonstrates the utmost importance of NF-I binding to the CCAAT box in FP-1 for proximal α1(I)pro-collagen promoter activity in HSC that appears to be a target of PPARγ.

PPARγ Inhibits NF-I but Not Sp1-mediated Stimulation of the −133 bp Collagen Promoter—To further test the effects of PPARγ on NF-I-mediated proximal promoter activity, transient transfection experiments were performed using the −133 promoter-reporter plasmid (pCOL−133) and an expression vector for NF-I, Sp1, or both in the absence or presence of PPARγ expression. We first examined the regulatory effects of NF-I and Sp1 on the promoter. For this purpose, we used NIH3T3 fibroblasts that have been previously used to characterize NF-I and Sp1 regulation of this specific promoter (19). A transient transfection experiment revealed that NF-I overexpression modestly but dose-dependently transactivated the pCOL−133 promoter. A mild 1.8-fold increase in promoter activity is achieved with 300 ng of NF-I plasmid, the maximum amount used for this experiment (Fig. 5*B*). On the other hand, Sp1 overexpression markedly increases the promoter activity as much as 350-fold with 400 ng of Sp1 (Fig. 5*C*). We also tested the combined effect of NF-I and Sp1 on the collagen promoter by co-transfecting with 100 ng each of both plasmids. This co-expression results in a synergistic induction of the promoter activity in NIH3T3 (Fig. 5*D*), and the same effect is also confirmed in BSCs (Fig. 5*E*). We then tested the effects of PPARγ on NF-I- or Sp1-mediated activation of the collagen promoter as well as the effect of PPARγ on the synergistic activation of this promoter by both factors. Our results show that PPARγ significantly inhibits NF-I-mediated promoter activity in NIH3T3 and BSCs (Fig. 5, *D* and *E*). In contrast and to our surprise, PPARγ does not inhibit Sp1 transactivity toward this promoter in either cell type (Fig. 5, *D* and *E*). In addition, PPARγ significantly reduces NF-I/Sp1 synergistic induction of the collagen promoter by in NIH3T3 and BSCs (Fig. 5, *D* and *E*). These results confirm NF-I as a primary target for the inhibitory effect of PPARγ on the proximal α1(I) collagen promoter.

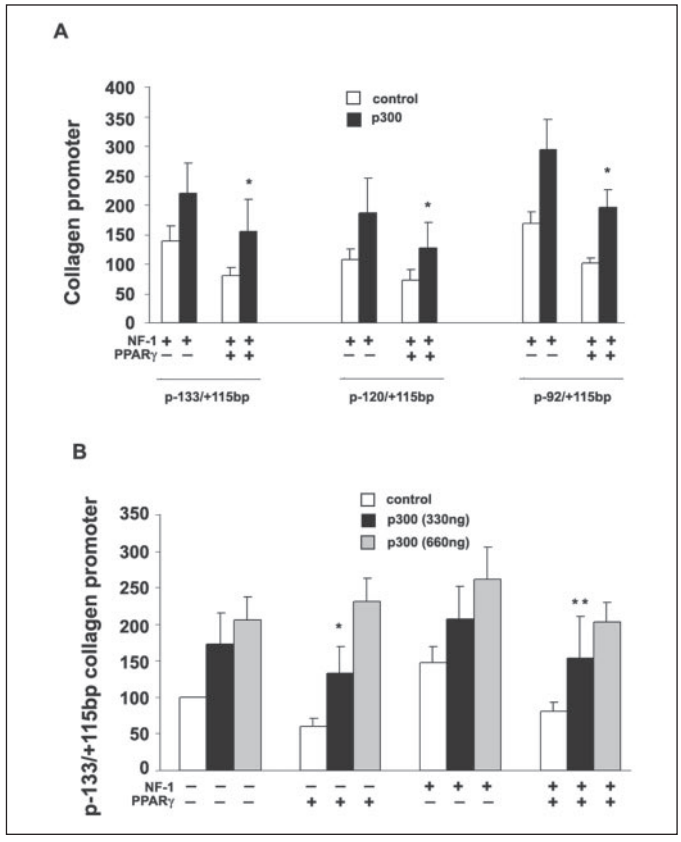

FIGURE 6. **p300 rescues NF-I from the inhibitory effect of PPARγ.** *A*, transfection with p300 (330 ng) partially rescues NF-I-mediated collagen promoter activity from inhibitory regulation by PPARγ. *, $p < 0.05$ compared with the control ($n = 3–5$) (without p300 overexpression) *B*, p300 dose-dependently reduces PPARγ suppression of NF-I-driven collagen promoter activity. *, $p < 0.05$ compared with the promoter activity without NF-I or PPARγ expression but with p300 transfection at 330 ng (*second bar* from *left*) ($n = 4–5$); **, $p < 0.05$ compared with the activity by the cells transduced with NF-I and 330 ng of p300 (*eighth lane* from *left*). *IP*, immunoprecipitation.

p300 Rescues the Inhibitory Effect of PPARγ on NF-I-mediated Collagen Promoter Activity—Our results demonstrate that PPARγ inhibits basal α1(I) procollagen promoter activity at the site upstream of −133 bp comprising overlapping NF-I and Sp1 sites. They also demonstrate that the promoter activity stimulated by NF-I but not Sp1 is inhibited by PPARγ, and this effect is probably due to reduced NF-I binding to FP-1. Since NF-I and PPARγ share common co-activators, such as p300, and a competition for p300 by PPARγ with other transcription factors is possible, we examined whether the inhibitory effect of PPARγ on NF-I involves p300. To address this question, we overexpressed p300 to determine its effects on PPARγ-mediated inhibition of NF-I-dependent promoter activity. Our results show that 330 ng of the p300 expression plasmid partially rescues NF-I from the inhibitory effect of PPARγ on each of the three collagen promoter deletion constructs tested, pCOL−133/+115bp, pCOL−120/+115bp, and pCOL-92/+115bp, suggesting the involvement of p300 within FP-1 (Fig. 6*A*). In addition, p300 dose-dependently relieves the suppression by PPARγ of basal pCOL−133 promoter activity (Fig. 6*B*, *second set* of *bar graphs*). More importantly, p300 dose-dependently rescues NF-I from the suppressive effect of PPARγ on the promoter (Fig. 6*B*, *third set* of *bar graphs*). Thus, these results suggest that PPARγ inhibits NF-I-mediated collagen promoter activity at least in part via competition between these two transcription factors for p300.

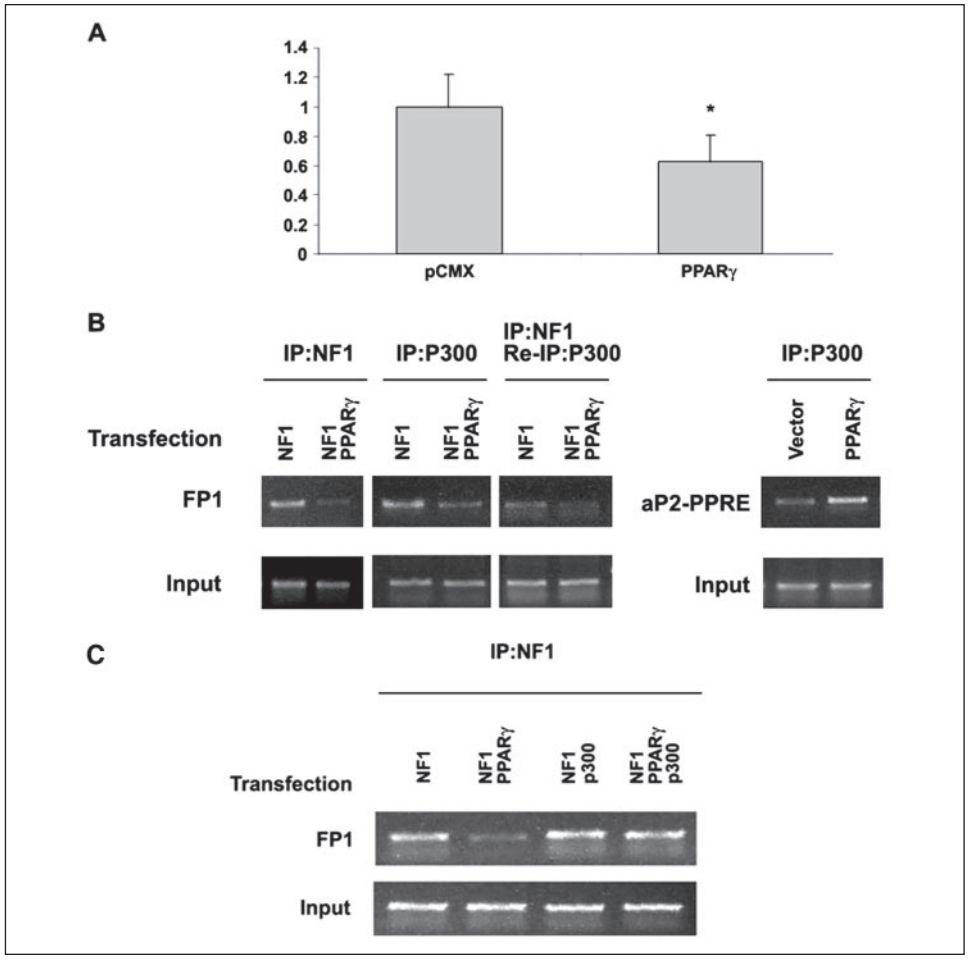

FIGURE 7. **PPARγ inhibits the binding of NF-I to FP-1 *in vivo* via suppression of p300-facilitated binding of NF-I to DNA.** *A*, basal NF-I binding to FP-1 is reduced by PPARγ. Transfection of NIH3T3 cells with a PPARγ expression vector reduces the binding of NF-I to FP-1 as determined by the ChIP assay and Syber Green real time PCR. *, $p = 0.026$ as compared with the cells transfected with the empty vector pCMX. *B*, the cells transfected with a NF-I expression vector show a distinct PCR band of FP-1 after immunoprecipitation with anti-NF-I antibody by ChIP assay (*first lane*), but this is reduced by PPARγ co-transfection (*second lane*), demonstrating inhibition of NF-I by PPARγ. P300 binding to FP-1 is also inhibited by PPARγ, as shown in the *third* and *fourth lanes*. The *fifth* and *sixth lanes* show that PPARγ inhibits p300 binding to FP-1 via NF-I as demonstrated by the two-step ChIP assay. The *last two lanes* serve to show a positive control for PPARγ by demonstrating increased p300 binding to the PPRE element in the aP2 gene by PPARγ overexpression. *C*, ChIP assay with NF-I immunoprecipitation shows that p300 transduction increases NF-I binding to FP-1 (*third lane versus first lane*) and completely abrogates PPARγ-mediated inhibition of NF-I binding (*fourth lane versus second lane*). These ChIP assays were repeated at least three times to determine the reproducibility of the results.

PPARγ Inhibits NF-I Binding to FP-1 in Vivo via Its Suppressive Effects on p300-stimulated NF-I-DNA Binding—We next tested whether PPARγ inhibits NF-I binding to FP-1 *in vivo* by the ChIP assay. First, using antibodies against NF-I and primers flanking FP-1, we amplified the FP-1 region that is bound with NF-I in NIH3T3 cells transduced 1) with or without PPARγ, 2) with NF-I with or without PPARγ. Under the basal condition (no NF-I overexpression), the amplified band for FP-1 in agarose gel is too weak to ascertain the effects of PPARγ. Thus, real time PCR using SyBer Green was performed to quantify the amplified FP-1 DNA. Using this technique, the binding of NF-I to FP-1 is shown to be reduced by 40% by PPARγ (Fig. 7*A*). ChIP assay also reveals NF-I binding to FP-1 under NF-I transduction is clearly inhibited by PPARγ (Fig. 7*B*, *lanes 1* and *2*). These results confirm the conclusion from our *in vitro* data obtained by EMSA (Fig. 4*E*). Next, we examined the binding of p300 to FP-1 by immunoprecipitating DNA with anti-p300 antibodies. As shown in the Fig. 7*B*, *lanes 3* and *4*, the p300 binding is coordinately suppressed by PPARγ. To determine whether p300 binding to FP-1 via NF-I is reduced, we performed a two-step ChIP assay. For this, we first immunoprecipitated DNA with anti-NF-I antibodies, followed by PCR and then reimmunoprecipitation with anti-p300 antibodies after a brief treatment with dithiothreitol for the second PCR. As shown in the *5th* and *6th lanes* of Fig. 7*B*, PPARγ reduces p300 association with FP-1 via NF-I. As a positive control for PPARγ transduction, we amplified the PPRE site for the aP2 gene after p300 immunoprecipitation. As shown in the *last two lanes* of Fig. 7*B*, transfection with the PPARγ vector expectedly increases the binding of p300 to the PPRE. These results may suggest that NF-I binding to FP-1 is reduced by PPARγ, and p300 recruitment to NF-I is consequently decreased. Then why does p300 overexpression rescue the PPARγ inhibitory effect on NF-I-driven promoter activity (Fig. 6)? Since the effect of PPARγ is mediated by suppressed NF-I binding, p300 must promote NF-I binding. This notion was tested by examining the effects of p300 on NF-I binding to FP-1 and on PPARγ-mediated inhibition of NF-I binding using the ChIP assay. Indeed, p300 promotes the binding of NF-I to FP-1 (Fig. 7*C*, *lane 3 versus lane 1*). Further, PPARγ-mediated inhibition of NF-I binding is prevented by p300 overexpression (Fig. 7*C*, *lane 2 versus lane 4*). These results suggest that PPARγ suppresses NF-I binding to FP-1 via its inhibition of p300-facilitated NF-I binding to its cognate binding site.

DISCUSSION

The present study identified a region proximal to −133 in the proximal 5′-flanking α1(I) procollagen promoter as the site of PPARγ-mediated inhibition. This region encompasses two known DNase footprints designated as FP-1 and FP-2 as determined using nuclear extracts from fibroblasts (19, 20) and activated HSC (24). Both footprints have reverse CCAAT binding sites and two identical 12-bp GC repeats (19). The CBF is shown to bind to the most proximal CCATT site of murine α2(I) procollagen promoter in NIH3T3 cells (25–27) and of human α1(I) procollagen promoter in skin fibroblasts (28). However, the primary proteins that are shown to bind to FP-2 are Sp1 and Sp3, and NF-I is shown to bind to the −100/−96 bp CCAAT box in FP-1 in both NIH3T3 cells and HSC (19, 24, 29). In fact, our EMSA and ChIP assays fail to demonstrate the binding of CBF to FP-1 in HSC despite the fact that CBF binding to the same site is evident in NIH3T3 cells (Fig. 4, *E*

and *F*) and skin fibroblasts (28). The literature suggests PPARγ causes negative cross-coupling with Sp1 as in the case for thromboxane receptor gene promoter activity in vascular smooth muscle cells (30). However, our transient transfection analysis and EMSA reveal inhibition of neither Sp1-induced pCOL−133α1(I) promoter activity nor Sp1 binding to FP-2 by PPARγ. Instead, both NF-I-stimulated promoter activity and NF-I-mediated synergistic induction of Sp1 transactivity are suppressed by PPARγ, demonstrating NF-I as a primary molecular target of PPARγ. To our knowledge, this is the first demonstration of negative regulation of NF-I by PPARγ. Our mutation experiment clearly demonstrates the utmost importance of the −100/−96 CCAAT site in FP-1 to the proximal promoter activity (Fig. 5*A*). Because of the very low activity of the mutated promoter, the effect of PPARγ could not be examined. However, it seems apparent from our data that PPARγ targets NF-I interaction with this CCAAT site. As we look into the underlying mechanisms, PPARγ is shown to inhibit NF-I binding to FP-1 as demonstrated by EMSA and ChIP assay. More importantly, this effect is mediated by suppression of p300-facilitated NF-I binding to its binding element as revealed by a reversal by p300 of the inhibitory effects of PPARγ on both the promoter activity (Fig. 6) and NF-I binding to FP-1 (Fig. 7*C*).

CBP/p300 are promiscuous co-activators that contribute to transcriptional activation by many transcription factors. They serve to recruit components of the general transcriptional machinery such as TFIID, TFIIB, and RNA polymerase. Its binding to activation domains of transcription factors brings histone acetyltransferases close to specific nucleosomes in target gene promoters (for a review, see Ref. 31). They also possess intrinsic acetyltransferase activity toward not only histones but also transcription factors. As exemplified by the regulation of p53 by p300, p300-mediated acetylation of transcription factors increases their binding to DNA (32). Our results also demonstrate a p300-mediated increase in NF-I binding to FP-1 of the proximal α1(I) procollagen promoter (Fig. 7*C*), and this mechanism is shown to be a target of the inhibitory action of PPARγ. p300 also interacts with multiple transcription factors to facilitate a synergism for transcriptional activation. In our study, synergism between NF-I and Sp1 is demonstrated for pCOL−133 activity, although NF-I alone has a modest stimulatory effect (Fig. 5*B*). Due to the overlapping binding sites for these two transcription factors in FP-1 and FP-2 and their proximity, this synergism is most likely facilitated by p300. If that were the case, PPARγ would readily reduce the synergistic activation of the collagen promoter by its inhibitory effect on p300. As demonstrated by the deletion analysis of the −220/+115 bp promoter, the intact FP-1 and FP-2 are required for the maximal PPARγ effect (Fig. 3*C*). Since the Sp1 and NF-I sites in FP-2 are disrupted in pCOL-120, the extent of inhibition is clearly attenuated (Figs. 3*C* and 5*A*). However, our EMSA data show the binding of Sp1 and Sp3 but not NF-I to FP-2 (Fig. 4*B*). Thus, these results suggest that the synergistic interaction of NF-I bound to FP-1 (Fig. 4*A*) and Sp1 bound to FP-2 is the target of PPARγ, and this is disrupted in the deletion construct pCOL-120. This specific aspect will need to be addressed further by our future study.

Although our study identifies NF-I as a target for PPARγ-mediated inhibition of the proximal α1(I)collagen promoter, our deletion analysis demonstrates that PPARγ still possesses a small inhibitory effect on pCOL-92 that has the proximal NF-I site disrupted (Figs. 3*C* and 5*A*). The absolute magnitude of this inhibition accounts only for 25% of the inhibition observed with pCOL−220 or pCOL−133. Nevertheless, this result still suggests an NF-I-independent mechanism for PPARγ-mediated inhibition. Indeed, the most proximal region upstream of −92 is known to have the binding sites for other proteins. For instance, YY-1, also known as NF-E1, binds to the element consisting of (C/t/a)CATN(T/a)(T/g/c) located at regions −40 to −34 bp and −35 to −29 bp of the α1(I) collagen promoter and up-regulates the transcription via stabilizing the interaction between TBP and TFIID and other components of the transcription machinery (33). YB-1, a member of the cold shock domain protein superfamily, binds to a specific DNA sequence (CTGATTGG) at −83 to −59 bp and inhibits the promoter activity due to its ability to separate DNA strands and to prevent the binding of other transcription factors (29). Thus, PPARγ may affect the binding or transcriptional regulation by these factors to render the observed inhibition of pCOL-92 activity. Further, PPARγ may also interact with other factors around the transcription start site, including the RFX family, that serve as repressors for both collagen type I genes (34).

In summary, the present study demonstrates that PPARγ reduces NF-I-mediated α1(I) collagen promoter activity via its ability to inhibit p300-facilitated binding of NF-I to DNA. The identification of the molecular target for PPARγ should aid in understanding the molecular basis of the antifibrotic effects mediated by PPARγ.

REFERENCES

1. Kochanek, K. D., Murphy, S. L., Anderson, R. N., and Scott, C. (2004) *Natl. Vital Stat. Rep.* **53,** 1–115
2. Friedman, S. L. (1993) *N. Engl. J. Med.* **328,** 1828–1835
3. Rojkind, M., Giambrone, M. A., and Biempica, L. (1979) *Gastroenterology* **76,** 710–719
4. Friedman, S. L. (1997) *J. Gastroenterol.* **32,** 424–430
5. Rojkind, M., Novikoff, P. M., Greenwel, P., Rubin, J., Rojas-Valencia, L., de Carvalho, A. C., Stockert, R., Spray, D., Hertzberg, E. L., and Wolkoff, A. W. (1995) *Am. J. Pathol.* **146,** 1508–1520
6. Skrtic, S., Wallenius, V., Ekberg, S., Brenzel, A., Gressner, A. M., and Jansson, J. O. (1999) *J. Hepatol.* **30,** 115–124
7. Miura, K., Nagai, H., Ueno, Y., Goto, T., Mikami, K., Nakane, K., Yoneyama, K., Watanabe, D., Terada, K., Sugiyama, T., Imai, K., Senoo, H., and Watanabe, S. (2003) *Biochem. Biophys. Res. Commun.* **311,** 415–423
8. Asahina, K., Sato, H., Yamasaki, C., Kataoka, M., Shiokawa, M., Katayama, S., Tateno, C., and Yoshizato, K. (2002) *Am. J. Pathol.* **160,** 2191–2205
9. Kinnman, N., Goria, O., Wendum, D., Gendron, M. C., Rey, C., Poupon, R., and Housset, C. (2001) *Lab. Invest.* **81,** 1709–1716
10. Suzuki, K., Fukutomi, Y., Matsuoka, M., Torii, K., Hayashi, H., Takii, T., Oomoto, Y., and Onozaki, K. (1993) *Int. J. Lepr. Other Mycobact. Dis.* **61,** 609–618
11. Armendariz-Borunda, J., Katayama, K., and Seyer, J. M. (1992) *J. Biol. Chem.* **267,** 14316–14321
12. Bachem, M. G., Sell, K. M., Melchior, R., Kropf, J., Eller, T., and Gressner, A. M. (1993) *Virchows Arch. B Cell Pathol. Incl. Mol. Pathol.* **63,** 123–130
13. Weiner, F. R., Giambrone, M. A., Czaja, M. J., Shah, A., Annoni, G., Takahashi, S., Eghbali, M., and Zern, M. A. (1990) *Hepatology* **11,** 111–117
14. Maher, J. J., Lozier, J. S., and Scott, M. K. (1998) *Am. J. Physiol.* **275,** G847–G853
15. Miyahara, T., Schrum, L., Rippe, R., Xiong, S., Yee, H. F., Jr., Motomura, K., Anania, F. A., Willson, T. M., and Tsukamoto, H. (2000) *J. Biol. Chem.* **275,** 35715–35722
16. Galli, A., Crabb, D. W., Ceni, E., Salzano, R., Mello, T., Svegliati-Baroni, G., Ridolfi, F., Trozzi, L., Surrenti, C., and Casini, A. (2002) *Gastroenterology* **122,** 1924–1940
17. She, H., Xiong, S., Hazra, S., and Tsukamoto, H. (2005) *J. Biol. Chem.* **280,** 4959–4967
18. Hazra, S., Xiong, S., Wang, J., Rippe, R. A., Krishna, V., Chatterjee, K., and Tsukamoto, H. (2004) *J. Biol. Chem.* **279,** 11392–11401
19. Nehls, M. C., Rippe, R. A., Veloz, L., and Brenner, D. A. (1991) *Mol. Cell. Biol.* **11,** 4065–4073
20. Rippe, R. A., Lorenzen, S. I., Brenner, D. A., and Breindl, M. (1989) *Mol. Cell. Biol.* **9,** 2224–2227
21. Tsukamoto, H., Cheng, S., and Blaner, W. S. (1996) *Am. J. Physiol.* **270,** G581–G586
22. Sung, C. K., She, H., Xiong, S., and Tsukamoto, H. (2004) *Am. J. Physiol.* **286,** G722–G729
23. Schreiber, E., Matthias, P., Muller, M. M., and Schaffner, W. (1989) *Nucleic Acids Res.* **17,** 6419
24. Rippe, R. A., Almounajed, G., and Brenner, D. A. (1995) *Hepatology* **22,** 241–251
25. Hatamochi, A., Paterson, B., and de Crombrugghe, B. (1986) *J. Biol. Chem.* **261,** 11310–11314
26. Oikarinen, J., Hatamochi, A., and de Crombrugghe, B. (1987) *J. Biol. Chem.* **262,** 11064–11070
27. Hatamochi, A., Golumbek, P. T., Van, S. E., and de Crombrugghe, B. (1988) *J. Biol. Chem.* **263,** 5940–5947

28. Saitta, B., Gaidarova, S., Cicchillitti, L., and Jimenez, S. A. (2000) *Arthritis Rheum.* **43,** 2219–2229
29. Norman, J. T., Lindahl, G. E., Shakib, K., En-Nia, A., Yilmaz, E., and Mertens, P. R. (2001) *J. Biol. Chem.* **276,** 29880–29890
30. Sugawara, A., Uruno, A., Kudo, M., Ikeda, Y., Sato, K., Taniyama, Y., Ito, S., and Takeuchi, K. (2002) *J. Biol. Chem.* **277,** 9676–9683
31. Vo, N., and Goodman, R. H. (2001) *J. Biol. Chem.* **276,** 13505–13508
32. Gu, W., and Roeder, R. G. (1997) *Cell* **90,** 595–606
33. Riquet, F. B., Tan, L., Choy, B. K., Osaki, M., Karsenty, G., Osborne, T. F., Auron, P. E., and Goldring, M. B. (2001) *J. Biol. Chem.* **276,** 38665–38672
34. Sengupta, P., Xu, Y., Wang, L., Widom, R., and Smith, B. D. (2005) *J. Biol. Chem.* **280,** 21004–21014